

Effect of photoelectron mean free path on the photoemission cross-section of Cu(111) and Ag(111) Shockley states

Jorge Lobo-Checa,¹ J. Enrique Ortega,^{2,3,4} Arantazu Mascaraque,^{5,6} Enrique G. Michel,⁷ and Eugene E. Krasovskii^{4,8,9}

¹Centre d'Investigació en Nanociència i Nanotecnologia, CIN2 (CSIC-ICN), Esfera UAB, Campus de la UAB, E-08193 Bellaterra, Spain

²Universidad del País Vasco, Departamento Física Aplicada I, E-20018 San Sebastián, Spain

³Centro de Física de Materiales CSIC/UPV-EHU-Materials Physics Center, Manuel Lardizabal 5, E-20018 San Sebastián, Spain

⁴Donostia International Physics Center (DIPC), Paseo Manuel Lardizabal 4, E-20018 Donostia-San Sebastián, Spain

⁵Departamento de Física de Materiales, Universidad Complutense de Madrid, E-28040 Madrid, Spain

⁶Unidad Asociada IQFR (CSIC)-UCM, E-28040 Madrid, Spain

⁷Departamento de Física de la Materia Condensada and Instituto Universitario de Ciencia de Materiales "Nicolás Cabrera", Universidad Autónoma de Madrid, E-28049 Madrid, Spain

⁸Universidad del País Vasco, Departamento Física Materiales, E-20018 San Sebastián, Spain

⁹IKERBASQUE, Basque Foundation for Science, E-48011 Bilbao, Spain

(Received 6 October 2011; published 13 December 2011)

The photoemission cross-section of Shockley states of Cu(111) and Ag(111) surfaces is studied over a wide range of photon energies. The constant initial-state spectra are very different for the two surfaces and show rich structure that does not follow the generally accepted nearly free electron model for the final state. Angle resolved photoemission data are interpreted within a one-step *ab initio* theory, revealing a multiple Bloch wave structure of photoemission final states. The inelastic scattering parameter—optical potential—is determined, and the energy dependence of the mean free path of the outgoing electron is calculated, which turns out to be the key for the understanding of the photoemission cross-section curve. These are essential steps for future exploration of wave function perturbations in the presence of surface nanostructures.

DOI: [10.1103/PhysRevB.84.245419](https://doi.org/10.1103/PhysRevB.84.245419)

PACS number(s): 79.60.Bm, 73.20.At

I. INTRODUCTION

Surface states in metals are defined as two-dimensional (2D) Bloch waves decoupled from the bulk; i.e., they feature exponentially decaying oscillations toward the interior of the crystal.^{1,2} The shape of the surface-state wave function in the perpendicular (\perp) direction is of particular importance in nanostructured systems, where such decaying tail can give rise to novel quantum properties.³ In thin overlayers the surface states may extend deep in the bulk so as to reach the buried substrate, allowing the scattering at deep heterointerfaces, which can bestow exotic properties to the surface electron, such as spin polarization.⁴ It is also essential to understand lateral scattering at surface defects and nano-objects, such as steps,⁵ which are known to induce an elastic or electrostatic perturbation a few layers below the surface atomic plane.⁶ Thus, a proper description of surface states must include its crystal momentum decomposition in the surface perpendicular direction.

The analysis of the k_{\perp} composition of the surface state can be carried out with angle resolved photoemission (ARPES) in the so-called constant-initial-state (CIS) mode, namely through the analysis of the photon-energy-dependent photoemission cross-section.⁷⁻¹² The common analysis of the cross-section curve is based on k_{\perp} conservation and nearly free electron (NFE) final state bands with constant inner potential, so that a resonance peak is expected at the fundamental k_{\perp} component of the surface state, with a peak width that equals its inverse penetration length. However, photoelectron cross-sections vary strongly from one substance to another and cannot be understood directly from the spectral density of the final states or from simple k_{\perp} conservation arguments.¹³ Even for the nominally simple aluminum or beryllium metals the one-step photoemission theory reveals a strong effect of

the final states,¹⁴⁻¹⁶ which is not explainable within the NFE approach. Indeed, the NFE approximation for the final state is a useful first guess for the energy of the photoemission intensity resonance. However, it ignores the scattering of the photoelectron by the crystal lattice, giving rise to wrong conclusions, such as the k_{\perp} composition of the surface state. As we will demonstrate here for the noble-metal surfaces of Cu(111) and Ag(111), the perpendicular component of the wave function may indeed be inferred from the photon-energy-dependent cross-section, but the analysis of the latter requires rigorous first-principles calculations.

In this paper we experimentally and theoretically investigate the photon-energy-dependent photoemission cross-section of the Shockley states of Cu(111) and Ag(111) surfaces. We have observed a wealth of fine structure that originates from the complicated non-free-electron-like band structure at high energies (final states). We present an explanation of the CIS spectra within a first-principles one-step photoemission theory. In Cu(111) the excellent agreement between theory and experiment allows us to rather accurately estimate the inelastic scattering rate of the photoelectron, i.e., the optical potential. For Ag(111) the double-peak structure of the CIS spectrum is accurately reflected in the calculation, making it possible to determine the relative location of two final-state branches, and hence their different self-energy shifts. The different decay lengths of the Cu(111) and Ag(111) surface states are shown to manifest themselves in the width of the CIS spectra.

II. EXPERIMENT

The ARPES measurements were carried out using p polarized light at two different synchrotron radiation laboratories:

the Swiss Light Source (SLS) at the Paul Scherrer Institut (Villigen, Switzerland) and the Synchrotron Radiation Center (SRC) in Stoughton (Wisconsin, USA). The COPHEE end station located at the SIS beamline of the SLS is equipped with a hemispherical channeltron analyzer which at room temperature and photon energy 30 eV gave an angular resolution better than $\pm 0.5^\circ$ and an overall energy resolution of 30 meV. The SRC data were acquired at the PGM beamline using a hemispherical Scienta SES200 analyzer with an overall energy and angular resolution of 25 meV and 0.1° , respectively.

We used Ag(111) and Cu(111) single crystals prepared in vacuum following standard ion sputtering plus annealing cycles until an intense and well-defined Shockley state was visible in the raw photoemission data. The Shockley state of Cu(111) and Ag(111) was measured in a broad photon energy range from 21 eV to at least 90 eV in steps of 2 to 5 eV

close to normal emission. The data acquisition for each surface was repeated at least twice and at different synchrotrons in order to overrule possible higher harmonic contamination of the surface-state intensity, as well as to discard nonlinear channel-plate response effects. Practically identical results were obtained from these experimental data sets. The data were acquired at room (300 K) and low temperature (150 K), but we observed no effect on the line shape of the photoemission cross-section curve, shown in Fig. 1(b).

For each photon energy the photoemission spectra were first normalized to the photon flux by scaling the intensity to the photoyield current, which is generated on a metallic mesh located across the path of the incoming beam. After this normalization procedure the spectra close to the surface-state band bottom, i.e., at $k_{\parallel} = 0$ [shown in Fig. 1(a)] were fitted using a single Lorentzian convoluted with a linear background and multiplied by a Fermi-Dirac distribution. The extracted area of the Lorentzian component from the fit was then used to plot the photon-energy-dependent intensity curve of the bottom of the Shockley state, shown in Fig. 1(b).

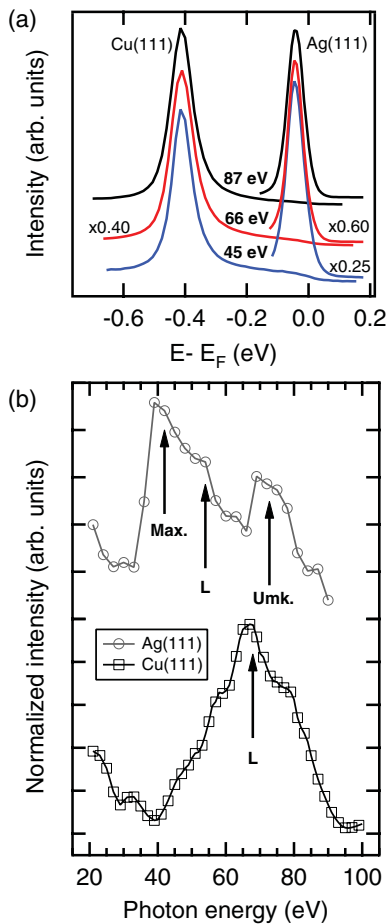


FIG. 1. (Color online) (a) Characteristic normal emission ARPES spectra and (b) photoemission cross section of the Shockley states of Ag(111) and Cu(111). The spectra of the surface-state minimum ($k_{\parallel} = 0$) were acquired at 150 K and present nondispersing peaks with photon energy at -0.045 eV for Ag(111) and -0.415 eV for Cu(111). Important photon-energy-dependent intensity modulations are observed after normalizing the data to the incoming photon flux, as shown in the bottom graph. The arrows indicate photon energy positions for the L bulk points, and the maximum (Max.) and Umklapp (Umk.) for the Ag(111) case. The lines between points are guides to the eye.

III. PHOTOEMISSION RESULTS

Figure 1(a) shows normal emission ARPES spectra of Ag(111) and Cu(111) for three different photon energies. Although the peak widths remain practically constant, strong intensity modulations of the normal emission spectra are directly observed (cf. side factors next to each spectrum). In Fig. 1(b) we can follow the changes of the area of the Lorentzian component for each photon energy after performing the normalization and fitting procedure described in the previous section. The overall line shapes of both Cu(111) and Ag(111) spectra agree with previous works,⁷⁻¹¹ but our higher ARPES resolution allows us to resolve fine details overlooked in the past.

In the case of Cu(111) [bottom curve in Fig. 1(b)] the photoemission cross-section peaks at 67 eV, which is the expected energy for the L point resonance in the NFE approach with constant inner potential.^{7,8,10} The overall width of 29 eV is substantially larger than that obtained in previous works,^{7,10} where the inverse of this width was used to calculate the decay length of the Cu(111) surface state (see Table I). Importantly, well-resolved shoulders in the wings of the broad peak are visible in our data that do not fit into the NFE approximation for the final state. Some of these features were already evident in previous published data, but barely discussed.^{7,10}

TABLE I. Decay length of the surface states of Cu(111) and Ag(111) calculated in this work in comparison with values derived from the analysis of photoemission cross-section curves that assumed a nearly free electron approach for final states.

	Decay Length		
	Ref. 9	Ref. 10	This Work
Cu(111)	4.0 Å	4.8 Å	5.9 Å
Ag(111)	8.7 Å	28.0 Å	8.8 Å

The photoemission cross-section of the Shockley state of Ag(111) has a more complex shape than Cu(111) [cf. Fig. 1(b)], reflecting the weakness of the NFE approach. The Ag(111) curve does not peak at its L bulk resonance, which, according to the inner potential framework, is expected at 54 eV.^{10,11} Instead, we observe two maxima, at 41 and 73 eV. Remarkably, Hsieh *et al.*¹⁰ and Kevan *et al.*⁹ only report two peaks: one at ~ 44 eV, attributed to an atomic resonance^{10,11} as it coincides with the Ag $5s$ orbital maximum,¹⁷ and another at ~ 54 eV, which corresponds to the bulk L point resonance for a direct transition. Notably, the peak observed at 73 eV is not reported in any of the previous works, although it is present in the raw data of Samsavar *et al.*¹¹ According to our calculations, this peak originates from an Umklapp process [see Fig. 2(b)], specifically the bulk reciprocal lattice vector $\mathbf{G} = (2\pi/a) \cdot (2, 2, 0)$, since the expected energy of this peak is at 74 eV.

IV. PHOTOEMISSION THEORY

The *ab initio* calculations of ARPES are performed within the one-step photoemission theory.¹⁸ The emission intensity at photon energy ω is determined by the transition probability between the surface state $|\psi\rangle$ of energy E_{ss} and the so-called

photoemission final state $|\Phi\rangle$. The latter is the time-reversed LEED (low-energy electron diffraction) state of energy $E_{fin} = E_{ss} + \hbar\omega$. For the normal emission the surface-parallel Bloch vector is $\mathbf{k}_{\parallel} = 0$. The LEED wave function is a scattering solution for a plane wave incident from vacuum. The inelastic scattering is described by an imaginary part $-iV_i$ (optical potential) added to the potential in the crystal half space, so that $|\Phi\rangle$ is a spatially decaying eigenfunction of a non-Hermitian Hamiltonian with a real eigenvalue E_{fin} . In the crystal half space, where the potential is periodic, the function $|\Phi\rangle$ is given by its partial waves or complex band structure (CBS) expansion: $|\Phi\rangle = \sum |\kappa_i\rangle$, where each Bloch wave $|\kappa_i\rangle$ (with a complex surface normal projection κ_i of the wave vector) satisfies the Schrödinger equation. Relative contributions of the Bloch waves $|\kappa_i\rangle$ can be characterized by the partial currents T_i transmitted by the waves into the crystal in the LEED experiment. Thus, from the LEED calculation we can infer which partial waves affect the escape of the photoelectron to the vacuum. The waves with largest T_i are highlighted by thick lines in Figs. 2(c) and 2(f). In order to understand the connection between the observed spectra and the band structure we shall also consider partial contributions $\langle \kappa_i | \hat{\mathbf{p}} | \psi \rangle$ to the dipole matrix element; see Figs. 2(b) and 2(e).

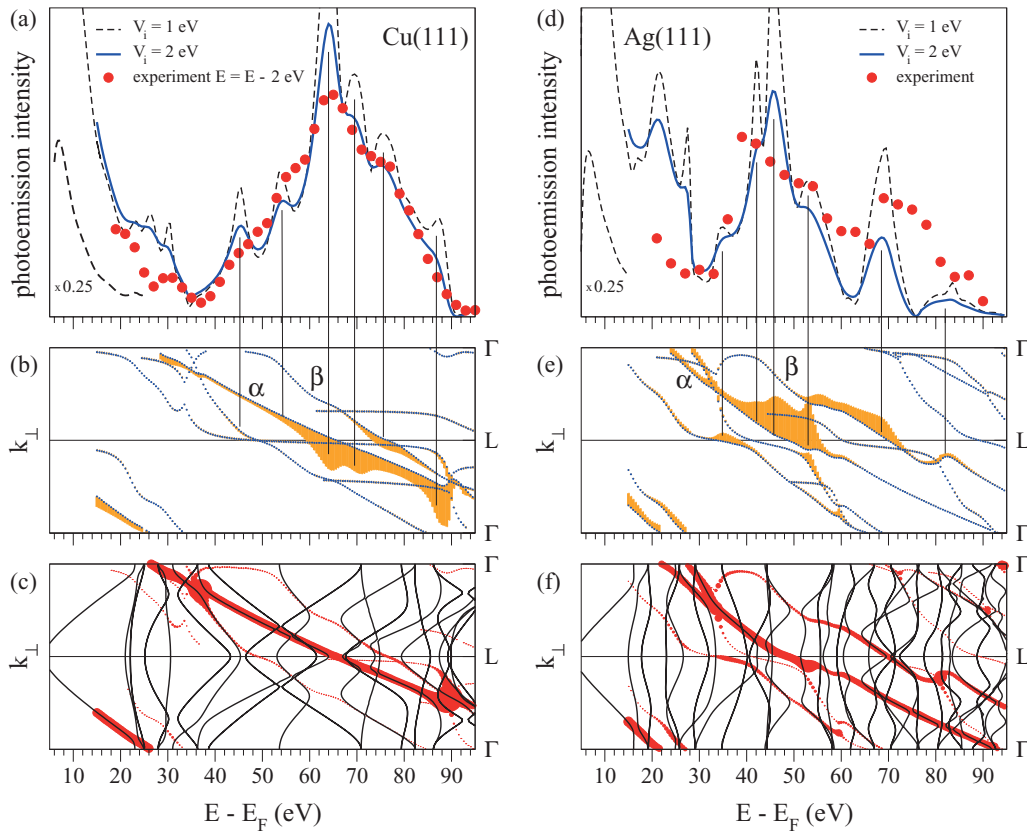


FIG. 2. (Color online) Complex band structure origin of the surface-state photoemission resonances for Cu(111) (left) and Ag(111) (right). (a) and (d) Experimental (from Fig. 1) dependence of the photoemission intensity on the final-state energy is shown by symbols. *Ab initio* one-step calculations are shown by lines: Solid lines are for $V_i = 2$ eV and dashed lines for $V_i = 1$ eV. (b) and (e) Partial Bloch wave decomposition of the emission intensity (α and β indicate the two main CBS branches) for $V_i = 2$ eV: Vertical extent of the shaded area is proportional to the squared modulus of the matrix element $|\langle \kappa_i | \hat{\mathbf{p}} | \psi \rangle|^2$. (c) and (f) Thin lines show real band structure (bulk states), and the thick line shows the conducting complex band structure. The thickness of the line is proportional to the current T_i carried by the individual partial wave.

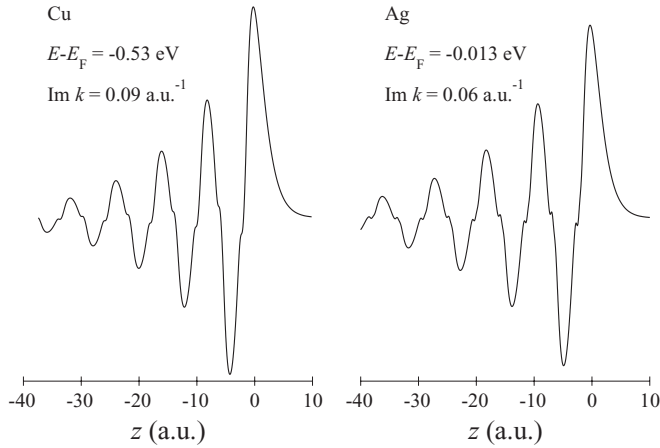


FIG. 3. The $G_{\parallel} = 0$ component of the surface-state wave functions. The decay lengths of the surface states are indicated in Table I and are extracted from the inverse of the imaginary part of the perpendicular momentum ($1/\text{Im}k_{\perp}$).

For the initial states the potential is assumed real. Because of the strong localization of the Ag(111) and Cu(111) surface states they are calculated in a repeated slab geometry (19 atomic layers). The final states are obtained as scattering solutions for a semi-infinite crystal with a step-like potential barrier between the bulk and the vacuum.¹⁹ The complex band structure is calculated with the inverse $\mathbf{k} \cdot \mathbf{p}$ method in the extended linear augmented plane wave formalism.²⁰ The crystal potential both at the surface (for the initial states) and in the bulk is determined self-consistently within the local density approximation (LDA) by the augmented Fourier components method.²¹

V. DISCUSSION

The noble metals Cu and Ag have a very similar electronic structure of the valence band, and the (111) surfaces of both crystals host a Shockley state close to the Fermi energy with very similar wave functions (see Fig. 3). It is interesting to compare the CIS spectra from the two states in order to understand similarities and differences in the structure of their final states. It is often thought that owing to the high kinetic energy of the outgoing photoelectron, the final states are only weakly affected by the crystal potential, so that the final state wave function can be fairly well approximated by a single plane wave.⁷ The comparison of the gross features of the CIS spectra from Cu(111) and Ag(111), however, suggests that this picture is oversimplified. Indeed, in Cu(111) it is a single broad maximum at 67 eV of 29 eV FWHM, whereas in Ag(111) two main maxima at 41 and 73 eV can be observed.

In both cases the photoemission signal is mainly generated from two CBS branches, α and β , although in Ag(111) other bands also contribute with considerable photocurrent, as observed in Figs. 2(b) and 2(e). As expected from the direct transitions picture the main peak appears close to the energy where k_{\perp} reaches the L point. However, because these energies lie within the gaps of the real band structure the surface-state photoemission cross-sections show a rather complicated behavior in both systems. In the case of Cu(111)

vertical transitions seem to dominate the spectrum. This explains why simple models can (by chance) give the correct energy of the main maximum and, therefore, qualitatively reproduce the experimental curves.⁷⁻¹⁰

On the contrary, the case of Ag(111) does not follow such a simple scenario. The L bulk resonance of the main final-state band does not stand out because there are partial Bloch waves which reduce, almost reaching its cancellation, the photocurrent due to the individual vertical transition *a priori* expected at ~ 54 eV. This makes the effective (calculated) cross-section maximum shift down to 45.8 eV, in fact very close to the measured ~ 42 eV photoemission intensity maximum indicated as “Max.” in Fig. 2(b). On the other hand, the final-state band responsible for the experimental peak at 73 eV can be regarded, as previously indicated, as an Umklapp since it closely follows the dispersion of the main final-state band but is displaced in energy [Figs. 2(e) and 2(f)]. We speculate that the observed Ag(111) cross-section contrasts with the apparent simplicity of Cu(111) because for the latter the transitions that give rise to the main maximum are closer to the L point than in the case of Ag, a fact possibly linked to the higher kinetic energy of these final states.

Table I compares the Shockley state wave function decay length obtained from the present *ab initio* calculations with those determined in previous works from the inverse width of the resonance peak of the photoemission cross-section curve.⁷⁻¹² The discrepancy is striking. The decay lengths of the surface-state wave functions from our calculations (Fig. 3) are $1/\text{Im}k_{\perp} = 5.9 \text{ \AA}$ for Cu(111) and $1/\text{Im}k_{\perp} = 8.8 \text{ \AA}$ for Ag(111). Only the value for Ag is close to the one obtained with the analysis of the cross-section curve in Ref. 9, but this coincidence appears accidental. As demonstrated in our calculations, many bands contribute to the overall experimental photoemission cross-section, which modifies its line shape. Therefore, the generally accepted final-state free-electron band picture is totally misleading, even for the simplest noble-metal cases, and the total width of the spectra has no straight relation to the wave function penetration depth.

Our theoretical method only uses a single adjustable parameter, namely the optical potential V_i , that can be varied to fit the energy dependence of the experimental photoemission cross section. Increasing the value of the optical potential V_i leads to a line-shape broadening in the calculated cross-section curve, but it does not alter the energy locations of the peaks and the characteristic overall shape of the curve [cf. full and dashed curves in Figs. 2(a) and 2(d)]. For both Cu(111) and Ag(111) the best agreement with the experimental cross-section curve is obtained with an energy-independent V_i of 2 eV, which is close to the values obtained for Al^{14,15} and Be.¹⁶ The optical potential determines the average mean free path of the outgoing electrons, but its energy variations $\lambda(E)$ depend on the band structure of the final states. Although the main conducting branches look similar for Cu(111) and Ag(111) [cf. Figs. 2(c) and 2(f)] the $\lambda(E)$ curves presented in Fig. 4 reveal a striking difference between the two surfaces. In particular, at the L point resonance in Cu(111) (around 65 eV) $\lambda(E)$ shows only a weak minimum, whereas in Ag(111) the minimum (around 50 eV) is much deeper, and the values of λ are considerably lower than for Cu(111). This, apparently, strongly reduces the intensity of the nominally direct transitions at the L point

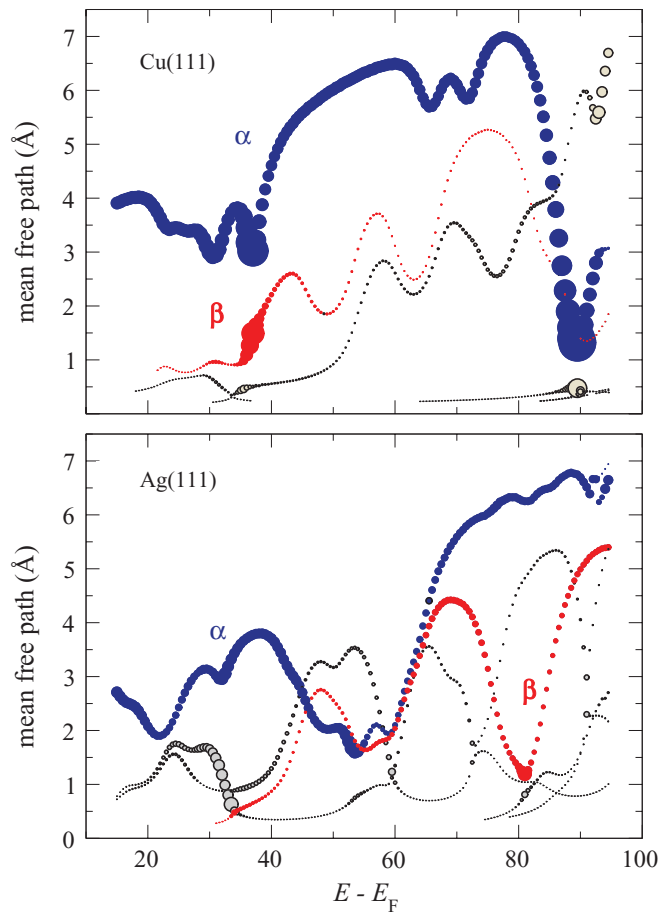


FIG. 4. (Color online) Energy dependence of the mean free path $\lambda = (2\text{Im}k_{\perp})^{-1}$ for several branches of the final-state complex band structure of Cu(111) and Ag(111). As in Figs. 2(c) and 2(f) it is $V_i = 2$ eV, and the size of the symbol is proportional to the current transmitted by the partial wave.

in Ag(111) and explains the very different shape of the CIS curves of the two surfaces.

At low photon energies [see the downscaled curves in Figs. 2(a) and 2(d)] the photoemission cross-section steadily grows with decreasing energy, similar to the behavior of the cross-section of the surface states on Al(100) and Be(0001) calculated in Ref. 16. This energy region was experimentally studied in Ref. 22 for Cu(111), and it was found that the ratio of the surface state to the upper d -band intensity decreases by more than two orders of magnitude in going from $h\nu = 8$ eV to 25 eV. The cross-section of the d states was assumed to vary smoothly with energy, and this pronounced change in the intensity ratio was ascribed to the sp character of the surface state. The present calculation shows that the cross-section calculated in the dipole approximation decreases by only a

factor of 7 over this energy interval. This emphasizes the effect of other surface-related aspects, which differently affect photoemission from surface and bulk states. First, at low photon energies the dielectric response of the crystal (both local and nonlocal) becomes important. Its implications for CIS spectra have been thoroughly investigated both experimentally^{23,24} and theoretically.^{16,25,26} The nonlocal response may lead to an enhancement of the exciting electric field in the close vicinity of the surface, which, naturally, differently influences strongly localized surface states and extended bulk states. In addition, the photoelectron mean free path becomes much larger at lower kinetic energies, which enhances the emission intensity from the extended states much stronger than for the surface states.

VI. CONCLUSIONS

By combining ARPES experimental data with *ab initio* calculations we are able to understand the complex photoemission cross-section of the Shockley states of Cu(111) and Ag(111). The generally accepted final-state free-electron band picture based on the NFE model fails to reproduce the fine details observed in Cu(111) and simply cannot follow the Ag(111) experimental data. In this work we demonstrate that the width of the photoemission cross-section curve has no straight relation to the wave function penetration depth, as often believed. The penetration depth of the Ag(111) Shockley state is longer (8.8 Å) than for Cu(111) (5.9 Å). For both materials the optical potential obtained is $V_i \sim 2$ eV, similar to aluminum or beryllium. Importantly, the differences observed in the photoemission cross-section at the L resonance between the two noble metals can be rationalized with the outgoing electron's mean free path, as calculated from the crystal band structure and the optical potential V_i . We find the present results particularly relevant for nanostructured systems, for example vicinal surfaces, where the resonant character of their surface states might be investigated through such kind of photoemission cross-section curves—in particular, the question of whether the surface state changes into a surface resonance when increasing the density of steps at the surface, which is still controversial.

ACKNOWLEDGMENTS

We acknowledge J. Osterwalder and T. Greber for their continuous support and also the help of the beamline staffs from both the SRC and SLS synchrotrons during experiments. This work was supported by the Spanish Ministerio de Ciencia e Innovación (Grants No. FIS2010-19609-C02-02, FIS2008-00399, MAT2010-21156-C03-01, and MAT2010-21156-C03-02 and through the Research Program *Ramón y Cajal*) and the Basque Government (IT-257-07). The SRC is funded by the National Science Foundation (Award No. DMR-0084402).

¹S. Hüfner, *Photoelectron Spectroscopy: Principles and Applications*, 3rd ed. (Springer, Berlin, 2003).

²P. M. Echenique, R. Berndt, E. V. Chulkov, Th. Fauster, A. Goldmann, and U. Höfer, *Surf. Sci. Rep.* **52**, 219 (2004).

³J. H. Dil, F. Meier, J. Lobo-Checa, L. Patthey, G. Bihlmayer, and J. Osterwalder, *Phys. Rev. Lett.* **101**, 266802 (2008).

⁴F. Schiller, R. Keyling, E. V. Chulkov, and J. E. Ortega, *Phys. Rev. Lett.* **95**, 126402 (2005).

- ⁵A. Mugarza and J. E. Ortega, *J. Phys. Condens. Matter* **15**, S3281 (2003).
- ⁶X. Y. Wang, X. J. Shen, and R. M. Osgood Jr., *Phys. Rev. B* **56**, 7665 (1997).
- ⁷S. G. Louie, P. Thiry, R. Pinchaux, Y. Pétrouff, D. Chandesris, and J. Lecante, *Phys. Rev. Lett.* **44**, 549 (1980).
- ⁸S. D. Kevan and R. H. Gaylord, *Phys. Rev. Lett.* **57**, 2975 (1986).
- ⁹S. D. Kevan and R. H. Gaylord, *Phys. Rev. B* **36**, 5809 (1987).
- ¹⁰T. C. Hsieh, P. John, T. Miller, and T. C. Chiang, *Phys. Rev. B* **35**, 3728 (1987).
- ¹¹A. Samsavar, T. Miller, and T. C. Chiang, *J. Phys. Condens. Matter* **2**, 1141 (1990).
- ¹²S. D. Kevan, *Phys. Rev. B* **34**, 6713 (1986).
- ¹³See for example A. Bansil and M. Lindroos, *Phys. Rev. Lett.* **83**, 5154 (1999); H. M. Fretwell *et al.*, *ibid.* **84**, 4449 (2000).
- ¹⁴E. E. Krasovskii and W. Schattke, *Phys. Rev. Lett.* **93**, 027601 (2004).
- ¹⁵E. E. Krasovskii, W. Schattke, P. Jiř íček, M. Vondráček, O. V. Krasovska, V. N. Antonov, A. P. Shpak, and I. Bartoš, *Phys. Rev. B* **78**, 165406 (2008).
- ¹⁶E. E. Krasovskii, V. M. Silkin, V. U. Nazarov, P. M. Echenique, and E. V. Chulkov, *Phys. Rev. B* **82**, 125102 (2010).
- ¹⁷J. Yeh and I. Lindau, *At. Data Nucl. Data Tables* **32**, 1 (1985).
- ¹⁸P. J. Feibelman and D. E. Eastman, *Phys. Rev. B* **10**, 4932 (1974).
- ¹⁹E. E. Krasovskii and W. Schattke, *Phys. Rev. B* **59**, 15609 (1999).
- ²⁰E. E. Krasovskii and W. Schattke, *Phys. Rev. B* **56**, 12874 (1997).
- ²¹E. E. Krasovskii, F. Starrost, and W. Schattke, *Phys. Rev. B* **59**, 10504 (1999).
- ²²J. A. Knapp, F. J. Himpsel, and D. E. Eastman, *Phys. Rev. B* **19**, 4952 (1979).
- ²³H. J. Levinson and E. W. Plummer, *Phys. Rev. B* **24**, 628 (1981).
- ²⁴R. A. Bartynski, E. Jensen, T. Gustafsson, and E. W. Plummer, *Phys. Rev. B* **32**, 1921 (1985).
- ²⁵N. Barberan and J. E. Inglesfield, *J. Phys. C* **14**, 3114 (1981).
- ²⁶P. J. Feibelman, *Prog. Surf. Sci.* **12**, 287 (1982).